The Hybrid Intelligent Method Based on Fuzzy Inference System and Its Application to Fault Diagnosis

Yaguo Lei
State Key Laboratory for Manufacturing Systems Engineering,
Xi'an Jiaotong University,
Xi'an
China

1. Introduction

Large-scale and complex mechanical equipments usually operate under complicated and terrible conditions such as heavy duty, erosion, high temperature, etc. Therefore, it is inevitable for the key components (bearings, gears and shafts, etc.) of these equipments to suffer faults with various modes and different severity degrees. However, faults of large-scale and complex mechanical equipments are characterized by weak response, multi-fault coupling, etc., and it is hard to detect and diagnose incipient and compound faults for these equipments.

One of the principal tools for diagnosing mechanical faults is vibration-based analysis [1–3]. Through the use of processing techniques of vibration signals, it is possible to obtain vital diagnosis information from the signals [4, 5]. Traditional fault diagnosis techniques are performed by diagnosticians observing the vibration signals and the spectra using their expertise and special knowledge. However, for mechanical equipments having complex structures, many monitoring cells and high degrees of automation, there is lots of data to be analyzed in the process of fault diagnosis. Obviously, it is impossible for diagnosticians to manually analyze so many data. Thus, the degree of automation and intelligence of fault diagnosis should be enhanced [6]. Researchers have applied artificial intelligent techniques to fault diagnosis of mechanical equipments, such as expert systems, fuzzy logic, neural networks, genetic algorithms, etc [7–10]. Correspondingly, prominent achievements have been obtained in the field of intelligent fault diagnosis. With the advancement of studies and applications, however, researchers find that individual intelligent techniques have their advantages and shortcomings as well. For incipient and compound faults of mechanical equipments, the diagnosis accuracy using an individual intelligent technique is quite low and the generalization ability is considerably weak. Thus, it is urgent and necessary to develop novel techniques and methods to solve these problems.

The combination of multiple intelligent techniques has been intensively studied to overcome the limitations of individual intelligent techniques and achieve better performance [11–13]. Multiple intelligent classifiers input different feature sets usually exhibit complementary classification behaviors. Thus, if the classification results of multiple intelligent techniques are combined to yield the final classification result, the final performance may be superior to the best performance of individual classifiers [14–16].

Based on the above analysis, a hybrid intelligent fault diagnosis method is presented in this chapter to diagnose incipient and compound faults of complex equipments. The method is developed by combining multiple adaptive neuro-fuzzy inference systems (ANFISs), genetic algorithms (GAs) and vibration signal processing techniques. The method employs signal preprocessing techniques to mine fault information embedded in vibration signals. Statistical features reflecting machinery health conditions from various aspects are synthesized to construct multiple feature sets and to fully reveal fault characteristics. Using an improved distance evaluation technique, the sensitive features are selected from all feature sets. Based on the independency and the complementary in nature of multiple ANFISs with different input feature sets, a hybrid intelligent method is constructed using GAs. The hybrid intelligent method is applied to fault diagnosis of rolling element bearings. The experimental results show the method based on multiple fuzzy inference systems is able to reliably recognize both incipient faults and compound faults.

The rest of this chapter is organized as follows. Section 2 presents the hybrid intelligent method based on fuzzy inference system. Feature extraction and selection, and adaptive neuro-fuzzy inference system are also introduced in this section. Section 3 gives two cases of fault diagnosis for rolling element bearings. The hybrid intelligent method is applied to diagnosing bearing faults and the corresponding results are reported. Section 4 compares the proposed hybrid intelligent method with individual intelligent methods in the light of classification accuracy, and further discusses the causes of the improvement produced by the hybrid method. Finally, conclusions are given in Section 5.

2. The hybrid intelligent method based on fuzzy inference system

The hybrid intelligent method is shown in Fig. 1. It includes the following five steps. First, vibration signals are filtered, and at the same time they are decomposed by empirical mode decomposition (EMD) and intrinsic mode functions (IMFs) are produced. The filtered signals and IMFs are further demodulated to calculate their Hilbert envelope spectra. Second, six feature sets are extracted. They are respectively time- and frequency-domain statistical features of both the raw and preprocessed signals. Third, each feature set is evaluated and a few sensitive features are selected from it by applying the improved distance evaluation technique. Correspondingly, six sensitive feature sets are obtained. Forth, each sensitive feature set is input into one classifier based on ANFIS for training and testing. There are altogether six different classifiers corresponding to the six sensitive feature sets. Fifth, the weighted averaging technique based on GAs is employed to combine the outputs of the six ANFISs and come up with the final diagnosis results.

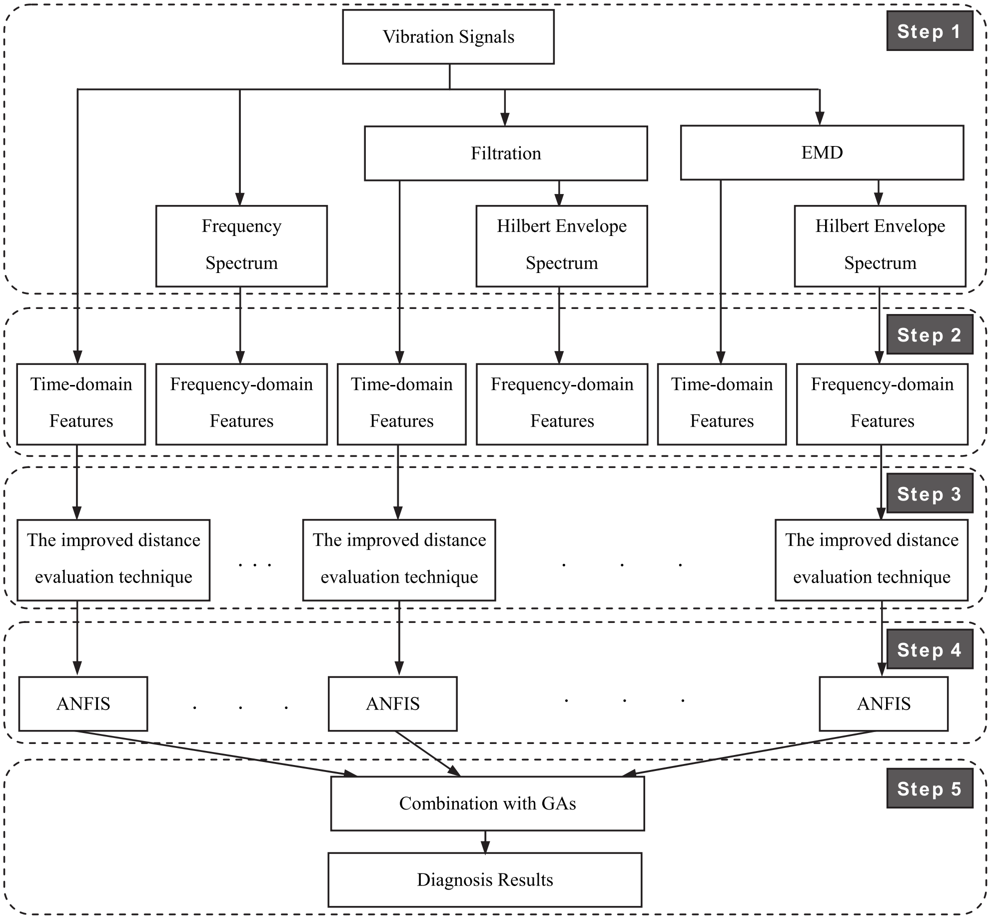

Fig. 1. Flow chart of the hybrid intelligent fault diagnosis method

2.1 Feature extraction

2.1.1 Statistical features of raw signals

Twenty-four feature parameters (p_1–p_{24}), presented in Table 1, are extracted [6] in this study. Eleven parameters (p_1–p_{11}) are time-domain statistical features and thirteen parameters (p_{12}–p_{24}) are frequency-domain ones. Once faults occur in mechanical equipments, the time-domain signal may change. Both its amplitude and distribution will be different from those of signals collected under healthy conditions. In addition, the frequency spectra and its distribution may change as well, which indicates that new frequency components appear and the convergence of frequency spectra varies. Parameter p_1 and p_3–p_5 reflect the vibration amplitude and energy in time domain. Parameter p_2 and p_6–p_{11} represent the time series distribution of the signal in time domain. Parameter p_{12} indicates the vibration energy in frequency domain. Parameter p_{13}–p_{15}, p_{17} and p_{21}–p_{24} describe the convergence of the spectrum power. Parameter p_{16} and p_{18}–p_{20} show the position change of major frequencies.

Time-domain feature parameters		Frequency-domain feature parameters	
$p_1 = \frac{\sum_{n=1}^{N} x(n)}{N}$	$p_7 = \frac{\sum_{n=1}^{N}(x(n)-p_1)^4}{(N-1)p_2^4}$	$p_{12} = \frac{\sum_{k=1}^{K} s(k)}{K}$	$p_{19} = \sqrt{\frac{\sum_{k=1}^{K} f_k^4 s(k)}{\sum_{k=1}^{K} f_k^2 s(k)}}$
$P_2 = \sqrt{\frac{\sum_{n=1}^{N}(x(n)-p_1)^2}{N-1}}$	$p_8 = \frac{p_5}{p_4}$	$p_{13} = \frac{\sum_{k=1}^{K}(s(k)-p_{12})^2}{K-1}$	$p_{20} = \frac{\sum_{k=1}^{K} f_k^2 s(k)}{\sqrt{\sum_{k=1}^{K} s(k) \sum_{k=1}^{K} f_k^4 s(k)}}$
$p_3 = \left(\frac{\sum_{n=1}^{N}\sqrt{\lvert x(n)\rvert}}{N}\right)^2$	$p_9 = \frac{p_5}{p_3}$	$p_{14} = \frac{\sum_{k=1}^{K}(s(k)-p_{12})^3}{K(\sqrt{p_{13}})^3}$	$p_{21} = \frac{p_{17}}{p_{16}}$
$p_4 = \sqrt{\frac{\sum_{n=1}^{N}(x(n))^2}{N}}$	$p_{10} = \frac{p_4}{\frac{1}{N}\sum_{n=1}^{N}\lvert x(n)\rvert}$	$p_{15} = \frac{\sum_{k=1}^{K}(s(k)-p_{12})^4}{Kp_{13}^2}$	$p_{22} = \frac{\sum_{k=1}^{K}(f_k-p_{16})^3 s(k)}{Kp_{17}^3}$
$p_5 = \max\lvert x(n)\rvert$	$p_{11} = \frac{p_5}{\frac{1}{N}\sum_{n=1}^{N}\lvert x(n)\rvert}$	$p_{16} = \frac{\sum_{k=1}^{K} f_k s(k)}{\sum_{k=1}^{K} s(k)}$	$p_{23} = \frac{\sum_{k=1}^{K}(f_k-p_{16})^4 s(k)}{Kp_{17}^4}$
$p_6 = \frac{\sum_{n=1}^{N}(x(n)-p_1)^3}{(N-1)p_2^3}$		$p_{17} = \sqrt{\frac{\sum_{k=1}^{K}(f_k-P_{16})^2 s(k)}{K}}$	$p_{24} = \frac{\sum_{k=1}^{K}(f_k-p_{16})^{1/2} s(k)}{K\sqrt{p_{17}}}$
		$p_{18} = \sqrt{\frac{\sum_{k=1}^{K} f_k^2 s(k)}{\sum_{k=1}^{K} s(k)}}$	
where $x(n)$ is a signal series for $n = 1, 2, \ldots, N$, N is the number of data points.		where $s(k)$ is a spectrum for $k = 1, 2, \ldots, K$, K is the number of spectrum lines; f_k is the frequency value of the kth spectrum line.	

Table 1. The feature parameters

Each vibration signal is processed to extract eleven time-domain features and thirteen frequency-domain features from its spectrum. The time- and frequency-domain features extracted here are hereafter referred as **feature set 1** and **feature set 2**, respectively. Therefore, feature sets 1 and 2 contain 11 and 13 feature values, respectively.

2.1.2 Statistical features of filtered signals

The examination of vibration signals indicates the presence of low-frequency interference. The signals are subjected to either high-pass or band-pass filtration to remove the low-frequency interference components. F filters are adopted and the selected filtration frequencies should completely cover the frequency components characterizing faults of mechanical equipments. The eleven time-domain features are extracted from each of the filtered signals. Therefore $11\times F$ time-domain features are obtained and defined as **feature set 3**.

In addition, the interference within the selected frequency band can be minimized by demodulation. Demodulation detection makes the diagnosis process a little more independent of a particular machine since it focuses on the low-amplitude high-frequency broadband signals characterizing machine conditions [17]. By performing demodulation and Fourier transform on the F filtered signals, we can obtain F envelope spectra. The envelope spectra are further processed to extract another set of $13\times F$ frequency-domain features. This feature set is referred as **feature set 4**.

2.1.3 Statistical features of IMFs

To extract more information, each of these raw signals is decomposed using the EMD method. EMD is able to decompose a signal into IMFs with the simple assumption that any signal consists of different simple IMFs [18]. For signal $x(t)$, we can decompose it into I IMFs $c_1, c_2, \ldots, c_I$ and a residue r_I, which is the mean trend of $x(t)$. The IMFs include different frequency bands ranging from high to low. The frequency components contained in each IMF are different and they change with the variation of signal $x(t)$, while r_I represents the central tendency of signal $x(t)$. A more detailed explanation of EMD can be found in Ref. [18].

Generally, first S IMFs containing valid information are selected to further analysis. Similar to the feature extraction method of the raw signals, the eleven features in time domain are extracted from each IMF. Then, we get an additional set of $11\times S$ time-domain features referred as **feature set 5**.

Each IMF is demodulated and its envelope spectrum is produced. We extract the thirteen frequency-domain features from the envelope spectrum and finally derive another set of $13\times S$ frequency-domain features defined as **feature set 6**.

2.2 Feature selection

Although the above features may detect faults occurring in mechanical equipments from different aspects, they have different importance degrees to identify different faults. Some features are sensitive and closely related to the faults, but others are not. Thus, before a feature set is fed into a classifier, sensitive features providing mechanical fault-related information need be selected to enhance the classification accuracy and avoid the curse of dimensionality as well. Here, an improved distance evaluation technique is presented and it is used to select the sensitive features from the whole feature set [6].

Suppose that a feature set of C machinery health conditions is

$$\{q_{m,c,j}, m=1,2,\ldots,M_c; c=1,2,\ldots,C; j=1,2,\ldots,J\}, \tag{1}$$

where $q_{m,c,j}$ is the *j*th eigenvalue of the *m*th sample under the *c*th condition, M_c is the sample number of the *c*th condition, and J is the feature number of each sample. We collect M_c samples under the *c*th condition. Therefore, for C conditions, we get $M_c \times C$ samples. For each sample, J features are extracted to represent the sample. Thus, $M_c \times C \times J$ features are obtained, which are defined as a feature set $\{q_{m,c,j}\}$.

Then the feature selection method based on the improved distance evaluation technique can be given as follows.

Step 1. Calculating the average distance of the same condition samples

$$d_{c,j} = \frac{1}{M_c \times (M_c - 1)} \sum_{l,m=1}^{M_c} \left| q_{m,c,j} - q_{l,c,j} \right|, \quad l,m=1,2,\ldots,M_c, l \neq m; \tag{2}$$

then getting the average distance of C conditions

$$d_j^{(w)} = \frac{1}{C} \sum_{c=1}^{C} d_{c,j}. \tag{3}$$

Step 2. Defining and calculating the variance factor of $d_j^{(w)}$ as

$$v_j^{(w)} = \frac{\max(d_{c,j})}{\min(d_{c,j})}. \tag{4}$$

Step 3. Calculating the average eigenvalue of all samples under the same condition

$$u_{c,j} = \frac{1}{M_c} \sum_{m=1}^{M_c} q_{m,c,j}; \tag{5}$$

then obtaining the average distance between different condition samples

$$d_j^{(b)} = \frac{1}{C \times (C-1)} \sum_{c,e=1}^{C} \left| u_{e,j} - u_{c,j} \right|, \quad c,e=1,2,\ldots,C, c \neq e. \tag{6}$$

Step 4. Defining and calculating the variance factor of $d_j^{(b)}$ as

$$v_j^{(b)} = \frac{\max(\left| u_{e,j} - u_{c,j} \right|)}{\min(\left| u_{e,j} - u_{c,j} \right|)}, \quad c,e=1,2,\ldots,C, c \neq e. \tag{7}$$

Step 5. Defining and calculating the compensation factor as

$$\lambda_j = \frac{1}{\dfrac{v_j^{(w)}}{\max(v_j^{(w)})} + \dfrac{v_j^{(b)}}{\max(v_j^{(b)})}} . \tag{8}$$

Step 6. Calculating the ratio of $d_j^{(b)}$ to $d_j^{(w)}$ and assigning the compensation factor

$$\alpha_j = \lambda_j \frac{d_j^{(b)}}{d_j^{(w)}} ; \tag{9}$$

then normalizing α_j by its maximum value and getting the distance evaluation criteria

$$\bar{\alpha}_j = \frac{\alpha_j}{\max(\alpha_j)} . \tag{10}$$

Clearly, larger $\bar{\alpha}_j$ ($j = 1,2,\ldots,J$) indicates that the corresponding feature is better to distinguish the C conditions. Thus, the sensitive features can be selected from the feature set $q_{m,c,j}$ according to the distance evaluation criteria $\bar{\alpha}_j$ from large to small.

2.3 Review of ANFIS

The adaptive neuro-fuzzy inference system (ANFIS) is a fuzzy Sugeno model of integration where the final fuzzy inference system is optimized using the training of artificial neural networks. It maps inputs through input membership functions and associated parameters, and then through output membership functions to outputs. The initial membership functions and rules for the fuzzy inference system can be designed by employing human expertise about the target system to be modeled. Then ANFIS can refine the fuzzy if-then rules and membership functions to describe the input/output behavior of a complex system. Jang [19] found that even if human expertise is not available it is possible to intuitively set up reasonable membership functions and then employ the training process of artificial neural networks to generate a set of fuzzy if-then rules that approximate a desired data set.

In order to improve the training efficiency and eliminate the possible trapping due to local minima, a hybrid learning algorithm is employed to tune the parameters of the membership functions. It is a combination of the gradient descent approach and least-squares estimate. During the forward pass, the node outputs advance until the output membership function layer, where the consequent parameters are identified by the least-squares estimate. The backward pass uses the back propagation gradient descent method to update the premise parameters, based on the error signals that propagate backward. More detailed description regarding ANFIS can be referred to Ref. [19].

2.4 The combination of multiple ANFISs

The hybrid intelligent method is implemented by combining multiple ANFISs using GAs. The idea of combining multiple classifiers into a committee is based on the expectation that the committee can outperform its members. The classifiers exhibiting different behaviors will provide complementary information each other. When they are combined, performance improvement will be obtained. Thus, diversity between classifiers is considered as one of the desired characteristics required to achieve this improvement. This diversity between classifiers can be obtained through using different input feature sets.

In this study, the six different feature sets have been extracted and the relevant six sensitive feature sets have been selected. ANFIS is used as the committee member. The weighted averaging technique is utilized to combine the six classifiers based on ANFIS, and the final classification result of the hybrid intelligent method is given as follows:

$$\hat{y}_n = \sum_{k=1}^{6} w_k \hat{y}_{n,k} \ , \quad n = 1,2,\ldots,N' \ , \quad k = 1,2,\ldots,6 \ , \tag{11}$$

subject to

$$\begin{cases} \sum_{k=1}^{6} w_k = 1, \\ w_k \geq 0, \end{cases} \tag{12}$$

where $\hat{y}_n$ and $\hat{y}_{n,k}$ represent the classification results of the *n*th sample using the hybrid intelligent method and the *k*th individual classifier respectively, w_k is the weight associated with the *k*th individual classifier, and N' is the number of all samples.

Here, the weights are estimated by using GAs to optimize the fitness function defined by Equation (13). Real-coded genomes are adopted and a population size of ten individuals is used starting with randomly generated genomes. The maximum number of generations 100 is chosen as the termination criterion for the solution process. Non-uniform-mutation function and arithmetic crossover operator [20] are used with the mutation probability of 0.01 and the crossover probability of 0.8, respectively.

$$f = \frac{1}{1+E} , \tag{13}$$

where E is root mean square training errors expressed as

$$E = [\frac{1}{N''} \sum_{n=1}^{N''} (y_n - \hat{y}_n)^2]^{\frac{1}{2}} \ , \quad n = 1,2,\ldots,N'' , \tag{14}$$

where y_n is the real result of the *n*th training sample, and N'' is the number of the training samples.

3. Applications to fault diagnosis of rolling element bearings

Rolling element bearings are core components of large-scale and complex mechanical equipments. Faults occurring in the bearings may lead to fatal breakdowns of mechanical equipments. Therefore, it is significant to be able to accurately and automatically detect and diagnosis the existence of faults occurring in the bearings. In this section, two cases of rolling element bearing fault diagnosis are utilized to evaluate the effectiveness of the hybrid intelligent method. One is fault diagnosis of bearing test rig from Case Western Reserve University (CWRU), which involves bearing faults with different defect sizes [21]. The other is fault diagnosis of locomotive rolling bearings having incipient and compound faults. The vibration signals were measured under various operating loads and different bearing conditions including different fault modes and severity degrees in both cases.

3.1 Case 1: Fault diagnosis of bearings of CWRU test rig

Faults were introduced into the tested bearings using the electron discharge machining method. The defect sizes (diameter, depth) of the three faults (outer race fault, inner race fault and ball fault) are the same: 0.007, 0.014 or 0.021 inches. Each bearing was tested under four different loads (0, 1, 2 and 3 hp). The bearing data set was obtained from the experimental system under four different health conditions: (1) normal condition; (2) with outer race fault; (3) with inner race fault; (4) with ball fault. Thus, the vibration data was collected from rolling element bearings under different operating loads and health conditions. More information regarding the experimental test rig and the data can be found in Ref. [21].

We conduct three investigations over three different data subsets (A–C) of the rolling element bearings. The detailed descriptions of the three data subsets are shown in Table 2. Data set A consists of 240 data samples of four health conditions (normal condition, outer race fault, inner race fault and ball fault) with the defect size of 0.007 inches under four various loads (0, 1, 2 and 3 hp). Each of the four health conditions includes 60 data samples. Data set A is split into two sets: 120 samples for training and 120 for testing. It is a four-class classification task corresponding to the four different health conditions.

Data set B also contains 240 data samples. 120 samples with the detect size of 0.021 inches are used as the training set. The remaining 120 samples with the detect size of 0.007 inches are identical with the 120 training samples of data set A and form the testing samples of data set B. The purpose of using this data set is to test the classification performance of the proposed method to incipient faults when it is trained by the serious fault samples.

Data set C comprises 600 data samples covering four health conditions and four different loads. Each fault condition includes three different defect sizes of 0.007, 0.014 and 0.021 inches, respectively. The 600 data samples are divided into 300 training and 300 testing instances. For data set C, in order to identify the severity degrees of faults, we solve the ten-class classification problem.

As mentioned in Section 2, the statistical features are extracted from the raw signal, filtered signal and IMF of each data sample. Three band-pass (BP1–BP3) and one high-pass (HP) filters are adopted for this bearing data. The band-pass frequencies (in kHz) of the BP1–BP3 filters are chosen as: BP1 (2.2–3.8), BP2 (3.0–3.8), and BP3 (3.0–4.5), respectively. The cut-off frequency of the HP filter is chosen as 2.2 kHz. These frequencies are selected to cover the frequency components representing bearing faults.

Data set	The number of training samples	The number of testing samples	Defect size of training/testing samples (inches)	Health conditions	Label of classification
A	30	30	0/0	Normal	1
	30	30	0.007/0.007	Outer race	2
	30	30	0.007/0.007	Inner race	3
	30	30	0.007/0.007	Ball	4
B	30	30	0/0	Normal	1
	30	30	0.021/0.007	Outer race	2
	30	30	0.021/0.007	Inner race	3
	30	30	0.021/0.007	Ball	4
C	30	30	0/0	Normal	1
	30	30	0.007/0.007	Outer race	2
	30	30	0.007/0.007	Inner race	3
	30	30	0.007/0.007	Ball	4
	30	30	0.014/0.014	Outer race	5
	30	30	0.014/0.014	Inner race	6
	30	30	0.014/0.014	Ball	7
	30	30	0.021/0.021	Outer race	8
	30	30	0.021/0.021	Inner race	9
	30	30	0.021/0.021	Ball	10

Table 2. Description of three data subsets

In order to demonstrate the enhanced performance of the hybrid intelligent method based on fuzzy inference system, the method is compared with individual classifiers based on ANFIS. Considering the computational burden, in each investigation, only four sensitive features are selected from each of the six feature sets using the improved distance evaluation technique and then input into the corresponding classifier. For data set A, distance evaluation criteria $\overline{\alpha}_j$ of the six feature sets are shown in Fig. 2. The diagnosis results of the four data sets are shown in Table 3 and Fig. 3, respectively.

Observing the results in Table 3 and Fig. 3, we can get the following interesting things.

1. For data set A, since this classification problem is relatively simple, both the six individual classifiers and the hybrid intelligent method achieve the high training and testing accuracy (100%). However, comparing the classification error of the hybrid intelligent method with those of the individual classifiers plotted in Fig. 4, we can see that the classification error of the hybrid intelligent method is the least.

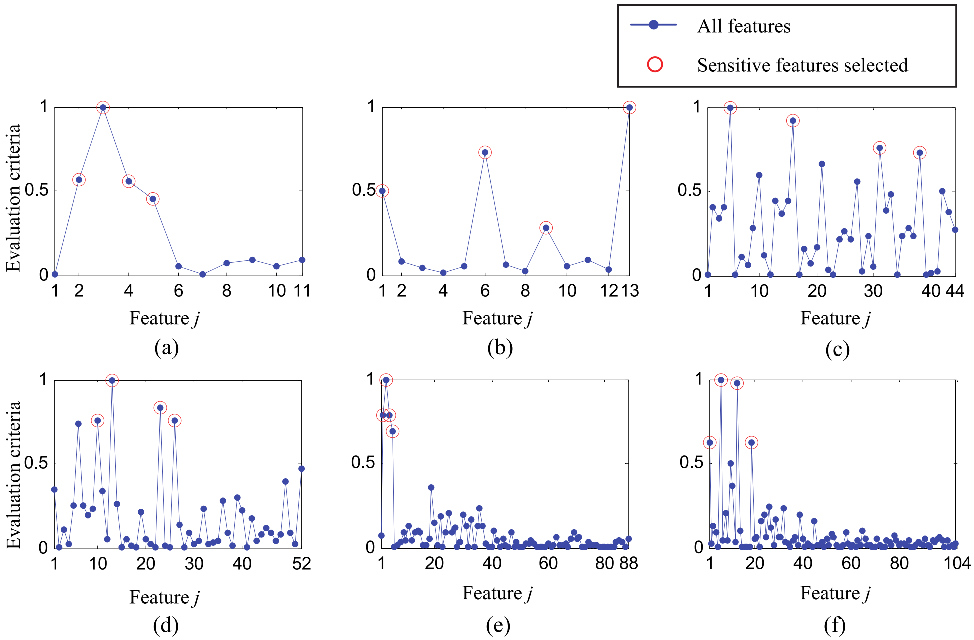

Fig. 2. Distance evaluation criteria of six feature sets of data set A: (a) feature set 1, (b) feature set 2, (c) feature set 3, (d) feature set 4, (e) feature set 5, and (f) feature set 6.

Data set	Classifier 1		Classifier 2		Classifier 3		Classifier 4	
	Training	Testing	Training	Testing	Training	Testing	Training	Testing
A	100	100	100	100	100	100	100	100
B	100	62.5	100	79.17	100	74.17	100	80
C	65.67	61	90	87.67	72.67	68	80.33	77

Data set	Classifier 5		Classifier 6		Average of six classifiers		Hybrid method	
	Training	Testing	Training	Testing	Training	Testing	Training	Testing
A	100	100	100	100	100	100	100	100
B	100	55.83	100	81.67	100	72.22	100	90.83
C	67.67	67	87.33	81	77.28	73.61	93.67	91.33

Table 3. Diagnosis results of the CWRU bearings using the hybrid intelligent classifier and individual classifiers

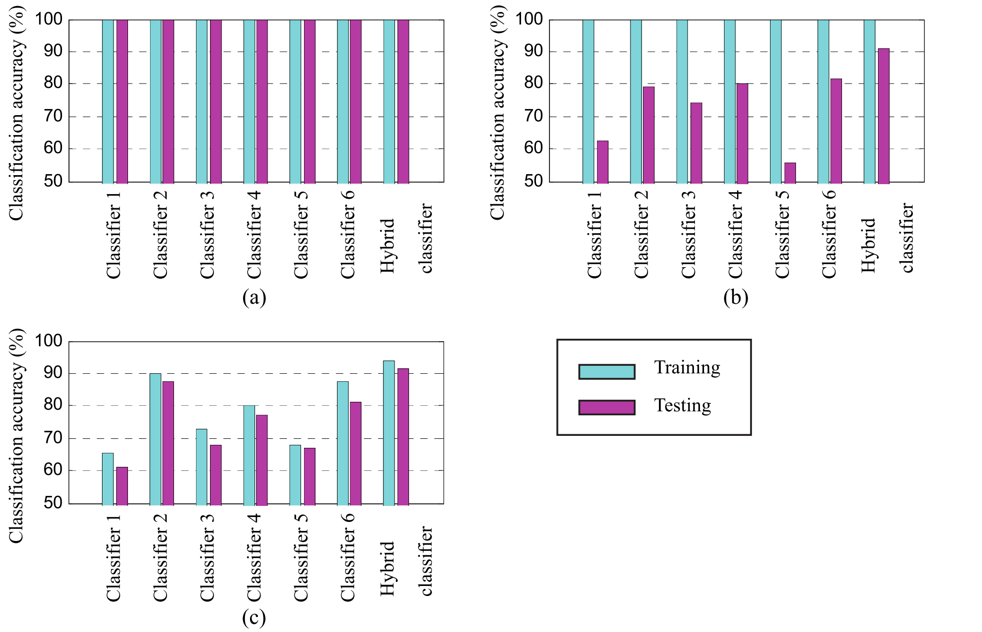

Fig. 3. Diagnosis results of the CWRU bearings: (a) data set A, (b) data set B, and (c) data set C.

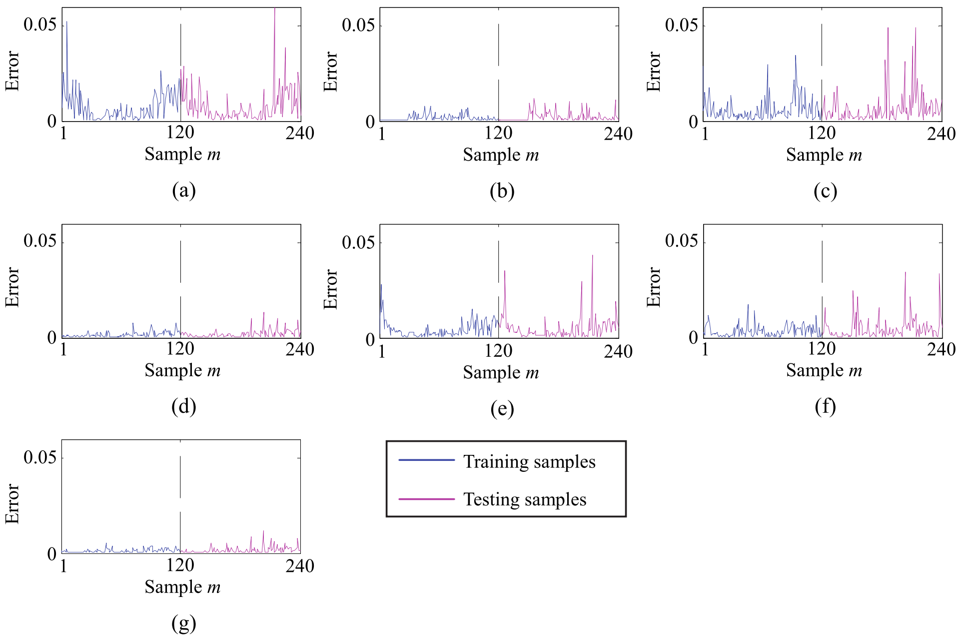

Fig. 4. Classification errors: (a) classifier 1, (b) classifier 2, (c) classifier 3, (d) classifier 4, (e) classifier 5, (f) classifier 6, and (g) the hybrid intelligent classifier.

2. For data set B, we can see that the training accuracies of all the classifiers are 100%. However, the hybrid intelligent method produces better testing performance (90.83%) than any of the individual classifiers ranging from 55.83% to 81.67% (average 72.22%). This result validates that the hybrid intelligent classifier trained by the serious fault data can diagnose the incipient faults with a higher accuracy in comparison with the individual classifiers.

3. For data set C, the training success rates of all the classifiers decrease and range from 65.67% to 93.67% because it is a ten-class classification problem and therefore relatively difficult. But the highest training accuracy (93.67%) is still generated by the hybrid intelligent method. For testing, the classification success of the six individual classifiers is in the range of 61–87.67% (average 73.61%), whereas the classification success of the hybrid method is much higher (91.33%). These imply that the hybrid method can identify both the different fault modes and the different fault severities better.

3.2 Case 2: Fault diagnosis of locomotive rolling bearings

The test bench of locomotive rolling bearings is shown in Fig. 5. The test bench consists of a hydraulic motor, two supporting pillow blocks (mounting with normal bearing), a tested bearing (52732QT) which is loaded on the outer race by a hydraulic cylinder, a hydraulic radial load application system, and a tachometer for shaft speed measurement. The bearing is installed in a hydraulic motor driven mechanical system. 608A11-type ICP accelerometers with a bandwidth up to 5 kHz are mounted on the load module adjacent to the outer race of the tested bearing for measuring its vibrations. The Advanced Data Acquisition and Analysis System by Sony EX is used to capture the vibration data. Parameters in the experiment are listed in Table 4.

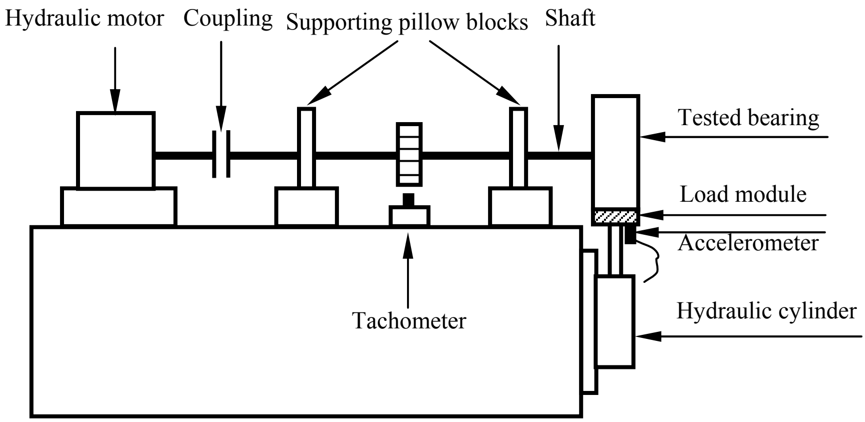

Fig. 5. Test bench of the locomotive rolling bearings.

A bearing data set containing nine subsets is obtained from the experimental system under the nine different health conditions. The nine conditions of bearings, shown in Table 5, involve not only incipient faults but also compound faults. The incipient faults are actually slight rub of outer races, inner races or rollers. These faulty bearings are shown in Fig. 6. Each data subset corresponds to one of the nine conditions and it consists of 50 samples.

Each sample is a vibration signal containing 8192 sampling points. Thus, the bearing data set includes altogether 450 data samples, which is divided into 225 training and 225 testing samples. This data is used to demonstrate the effectiveness of the proposed hybrid intelligent method in simultaneously identifying incipient faults and compound ones.

Parameter	Value
Bearing specs	52732QT
Load	9800N
Inner race diameter	160mm
Outer race diameter	290mm
Roller diameter	34mm
Roller number	17
Contact angle	0°
Sampling frequency	12.8 kHz

Table 4. Parameters in the experiment

Condition	Rotating speed	Label
Normal condition	About 490 rpm	1
Slight rub fault in the outer race	About 490 rpm	2
Serious flaking fault in the outer race	About 480 rpm	3
Slight rub fault in the inner race	About 500 rpm	4
Roller rub fault	About 530 rpm	5
Compound faults in the outer and inner races	About 520 rpm	6
Compound faults in the outer race and rollers	About 520 rpm	7
Compound faults in the inner race and rollers	About 640 rpm	8
Compound faults in the outer and inner races and rollers	About 550 rpm	9

Table 5. Health conditions of the locomotive rolling bearings

Two band-pass (BP1 and BP2) and one high-pass (HP) filters are used to filter the vibration signals of locomotive rolling bearings. The band-pass frequencies (in kHz) of the BP1 and BP2 filters are chosen as 1.5–2.7 and 1.5–4, respectively. The cut-off frequency of the HP filter is chosen as 3kHz. Similar to case 1, four sensitive features are selected from each of the six feature sets using the improved distance evaluation technique and then input into the corresponding classifier. The classification results of the hybrid intelligent method and six individual classifiers are shown in Fig. 7.

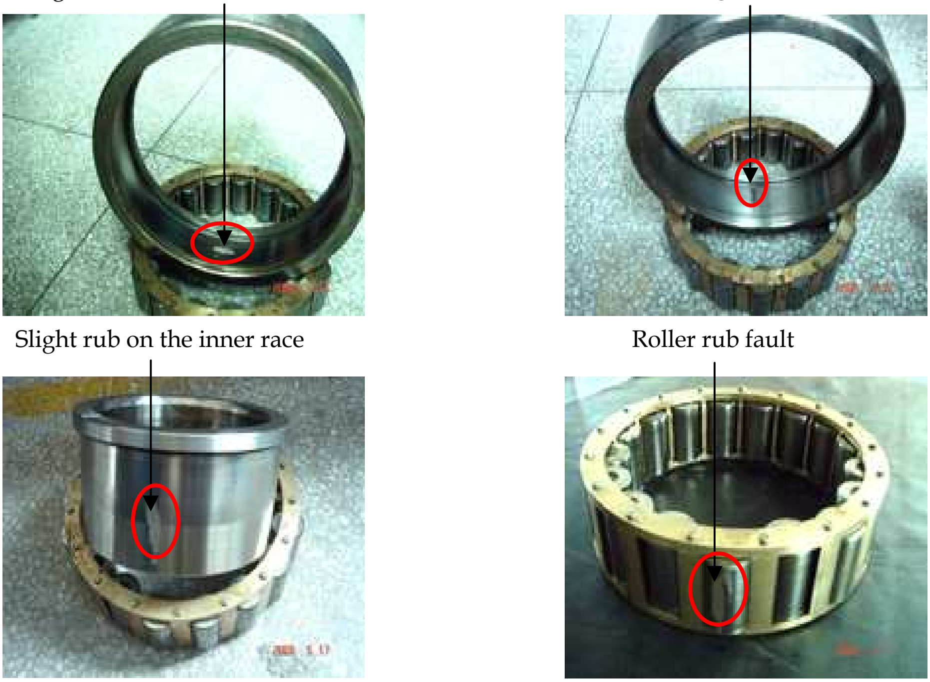

Fig. 6. Faults in the locomotive rolling bearings.

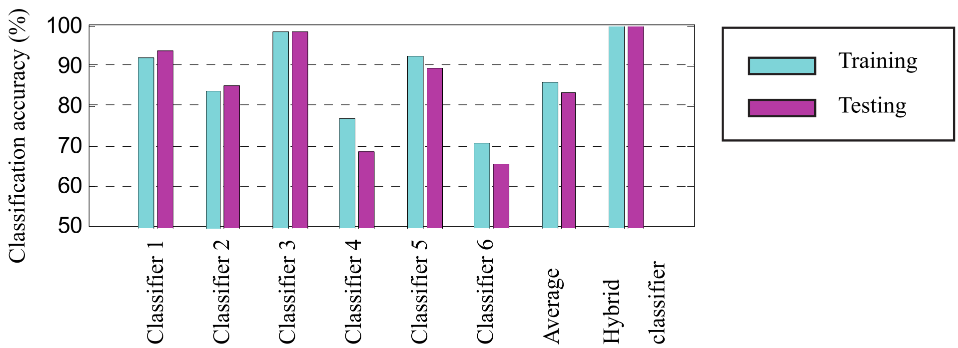

Fig. 7. Diagnosis results of the locomotive rolling bearings.

It is seen that the training accuracies of six individual classifiers are from 70.67% to 98.60% (average 85.69%) and the testing accuracies from 65.33% to 98.60% (average 83.39%). For the proposed hybrid intelligent method, however, both the training and testing accuracies are 100%. This result shows that the hybrid method achieves obvious improvements in recognition accuracy and provides a better generalization capability compared to the individual classifiers. Therefore, it is able to effectively identify not only incipient faults but also compound faults of locomotive rolling bearings.

4. Discussions

1. Comparing the diagnosis results of the proposed hybrid intelligent method with those of individual classifiers, we find that the testing accuracies of the hybrid intelligent method (100% for data set A, 90.83% for data set B and 91.33% for data set C in case 1; 100% in case 2) increase by 0, 18.61%, 17.72% and 16.61% compared with the average accuracies of the six individual classifiers. In addition, although the highest classification accuracy (100%) is obtained by all the classifiers for data set A in case 1, the classification error of the hybrid intelligent method is least among all classifiers. Thus, the proposed hybrid intelligent method is superior to the individual classifiers in the light of the classification accuracies.

2. All the above comparisons prove that the proposed hybrid intelligent method obtains significant improvements in fault diagnosis accuracy compared to the individual classifiers. It reliably recognizes both incipient faults and compound faults of rolling element bearings. The success obtained by the hybrid intelligent method may be attributed to the following three points. 1) Extracting both time- and frequency-domain features better reflects the machinery health conditions. 2) Selecting the sensitive features reflecting the fault characteristics avoids interference of other fault-unrelated features. 3) Combining multiple intelligent classifiers based on fuzzy inference system raises diagnosis accuracy.

3. The problems studied in this chapter cover single fault diagnosis, incipient fault diagnosis and compound fault diagnosis, and therefore they are typical cases of machinery fault diagnosis. The satisfactory experiment results demonstrate the effectiveness and generalization ability of the hybrid intelligent method. Although the proposed method is applied to fault diagnosis of the rolling element bearings successfully, it may also be employed to fault diagnosis of other rotating machinery.

5. Conclusions

In this chapter, a hybrid intelligent method based on fuzzy inference system is proposed for intelligent fault diagnosis of rotating machinery. In the method, several preprocessing methods, like empirical mode decomposition (EMD), filtration and demodulation, are utilized to mine fault information from vibration signals. In order to remove the redundant and irrelevant information, an improved distance evaluation technique is presented and used to select the sensitive features. Multiple fuzzy inference systems are combined using genetic algorithms (GAs) to enhance fault identification accuracy. The experimental results show that the hybrid intelligent method enables the identification of incipient faults and at the same time recognition of compound faults.

6. Acknowledgements

This research is supported by National Natural Science Foundation of China (51005172), the Fundamental Research Funds for the Central Universities and the Preferred Support Funds of the Scientific Research Project of the Ministry of Human Resources and Social Security of China for Returned Scholars.

7. References

[1] V. Indira, R. Vasanthakumari, V. Sugumaran, Minimum sample size determination of vibration signals in machine learning approach to fault diagnosis using power analysis, Expert Systems with Applications 37 (2010) 8650–8658.

[2] E. P. de Moura, C. R. Souto, A. A. Silva, et al., Evaluation of principal component analysis and neural network performance for bearing fault diagnosis from vibration signal processed by RS and DF analyses, Mechanical Systems and Signal Processing 25 (2011) 1765–1772.

[3] N. R. Sakthivel, V. Sugumaran, S. Babudevasenapati, Vibration based fault diagnosis of monoblock centrifugal pump using decision tree, Expert Systems with Applications 37 (2010) 4040–4049.

[4] Y. G. Lei, Z. J. He, Y. Y. Zi, et al., New clustering algorithm-based fault diagnosis using compensation distance evaluation technique, Mechanical Systems and Signal Processing 22 (2008) 419–435.

[5] S. J. Loutridis, Self-similarity in vibration time series: application to gear fault diagnostics, Transactions of the ASME, Journal of vibration and acoustics 130 (2008) 1–9.

[6] Y. G. Lei, Z. J. He, Y. Y. Zi, et al., Fault diagnosis of rotating machinery based on multiple ANFIS combination with GAs, Mechanical Systems and Signal Processing 21 (2007) 2280-2294.

[7] Y. G. Lei, Z. J. He, Y. Y. Zi, A new approach to intelligent fault diagnosis of rotating machinery, Expert Systems with Applications 35 (2008) 1593–1600.

[8] K. Mollazade, H. Ahmadi, M. Omid, et al., An intelligent model based on data mining and fuzzy logic for fault diagnosis of external gear hydraulic pumps, Insight 51 (2009) 594–600.

[9] Y. G. Lei, Z. J. He, Y. Y. Zi, Application of an intelligent classification method to mechanical fault diagnosis, Expert Systems with Applications 36 (2009) 9941-9948.

[10] B. Samanta, C. Nataraj, Use of particle swarm optimization for machinery fault detection, Engineering Applications of Artificial Intelligence, 22 (2009) 308–316.

[11] S. Rasheed, D. Stashuk, M. Kamel, Fusion of multiple classifiers for motor unit potential sorting, Biomedical Signal Processing and Control 3 (2008) 229–243.

[12] Y. Bi, J. Guan, D. Bell, The combination of multiple classifiers using an evidential reasoning approach, Artificial Intelligence 172 (2008) 1731–1751.

[13] F. Huenupán, N. B. Yoma, C. Molina, Confidence based multiple classifier fusion in speaker verification, Pattern Recognition Letters 29 (2008) 957–966.

[14] Y. G. Lei, Z. J. He, Y. Y. Zi, A combination of *W*KNN to fault diagnosis of rolling element bearings, Transactions of the ASME, Journal of Vibration and Acoustics 131 (2009) 1-6.

[15] A. K. J. Mohammad, R. Langari, A hybrid intelligent system for fault detection and sensor fusion, Applied Soft Computing, 9 (2009) 415–422.

[16] Y. G. Lei, M. J. Zuo, Z. J. He, et al., A multidimensional hybrid intelligent method for gear fault diagnosis, Expert Systems with Applications 37 (2010) 1419-1430.

[17] U. Benko, J. Petrovčič, D. Juričić, et al., An approach to fault diagnosis of vacuum cleaner motors based on sound analysis, Mechanical Systems and Signal Processing 19 (2005) 427–445.

[18] N. E. Huang, Z. Shen, S. R. Long, The Empirical mode decomposition and the Hilbert spectrum for nonlinear and non-stationary time series analysis, Proceedings of the Royal Society of London 454 (1998) 903–995.
[19] J. S. R. Jang, ANFIS: adaptive-network-based fuzzy inference system, IEEE Transactions on Systems, Man, Cybernetics 23 (1993) 665–685.
[20] Z. Michalewicz, Genetic Algorithms + Data Structures = Evolution Programs, 3rd Edition, Springer, NY, USA, 1999.
[21] X. S. Lou, K. A. Loparo, Bearing fault diagnosis based on wavelet transform and fuzzy inference, Mechanical Systems and Signal Processing 18 (2004) 1077–1095.

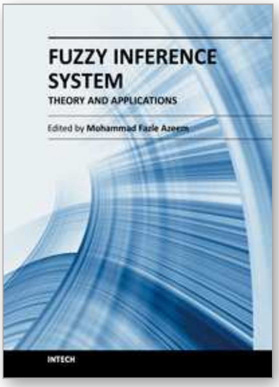

Fuzzy Inference System - Theory and Applications
Edited by Dr. Mohammad Fazle Azeem

ISBN 978-953-51-0525-1
Hard cover, 504 pages
Publisher InTech
Published online 09, May, 2012
Published in print edition May, 2012

This book is an attempt to accumulate the researches on diverse inter disciplinary field of engineering and management using Fuzzy Inference System (FIS). The book is organized in seven sections with twenty two chapters, covering a wide range of applications. Section I, caters theoretical aspects of FIS in chapter one. Section II, dealing with FIS applications to management related problems and consisting three chapters. Section III, accumulates six chapters to commemorate FIS application to mechanical and industrial engineering problems. Section IV, elaborates FIS application to image processing and cognition problems encompassing four chapters. Section V, describes FIS application to various power system engineering problem in three chapters. Section VI highlights the FIS application to system modeling and control problems and constitutes three chapters. Section VII accommodates two chapters and presents FIS application to civil engineering problem.

INTECH
open science | open minds

InTech Europe
University Campus STeP Ri
Slavka Krautzeka 83/A
51000 Rijeka, Croatia
Phone: +385 (51) 770 447
Fax: +385 (51) 686 166
www.intechopen.com

InTech China
Unit 405, Office Block, Hotel Equatorial Shanghai
No.65, Yan An Road (West), Shanghai, 200040, China
中国上海市延安西路65号上海国际贵都大饭店办公楼405单元
Phone: +86-21-62489820
Fax: +86-21-62489821